Journal of Sound and Vibration (1999) **220**(4), 601–624
Article No. jsvi.1998.1922, available online at http://www.idealibrary.com on IDEAL

A NEW DYNAMIC FINITE ELEMENT (DFE) FORMULATION FOR LATERAL FREE VIBRATIONS OF EULER–BERNOULLI SPINNING BEAMS USING TRIGONOMETRIC SHAPE FUNCTIONS

S. M. Hashemi and M. J. Richard

Department of Mechanical Engineering, Laval University, Québec, Québec, Canada G1K 7P4

and

G. Dhatt

Institut de Mécanique de Rouen, l'INSA de Rouen, 76131 *Mont Saint Aignan, France*

(*Received* 9 *July* 1997, *and in final form* 31 *July* 1998)

This paper presents a new Dynamic Finite Element (DFE) formulation for the vibrational analysis of spinning beams. A non-dimensional formulation is adopted, and the frequency dependent trigonometric shape functions are used to find a simple frequency dependent element stiffness matrix which has both mass and stiffness properties. An appropriate bisection method, based on a Sturm sequence root counting technique, is used and the flexural natural frequencies of cantilevered beams, for a variety of configurations, are studied. The results are compared to those found by the Dynamic Stiffness Matirx and the classical Finite Elements Method, using "Hermite" beam elements. Much better convergency rates are found using the proposed DFE method.

1. INTRODUCTION

The computation of natural frequencies and mode shapes are important elements in the dynamic analysis of rotating (centrifugally-stiffened) beams. The refinement of formulation techniques has led to the development of many studies on the vibration of rotating radial beams having different root offset configurations. This has been set in a variety of contexts ranging from turbomachinery blading and helicopter blades to gyroscopic instruments and flexible appendages on spinning spacecraft, etc. Numerous investigators have studied such structures and a variety of methods are proposed [1–14]. Some good literature surveys were presented on several occasions in the literature (see for example reference [8]). One can also find in reference [15] a review of several approximate methods such as the Mykelstad

0022–460X/99/090601 + 24 $30.00/0

method, the Galerkin method, the Rayleigh–Ritz method, the finite element method, etc.

1.1. FINITE ELEMENT METHOD (FEM)

The Finite Element Method (FEM), where beam element matrices are evaluated from assumed fixed shape functions, has been used by numerous investigators [6–10]. In standard FEM formulations, because of their completeness and ease of manipulation, polynomial shape functions are often used. The employment of polynomial shape functions, in this case, results in approximate equations in the form of mass and static stiffness matrices. However, in this case, the free vibrations analysis of a rotating beam, leads to the eigenvalue system

$$([K] - \omega^2[M])\{w\} = [K_{DS}]\{w\} = \{0\}, \tag{1}$$

which is linear in ω^2, and can be solved by different numerical methods. See, for example, reference [16].

A deviation from this practice will pay dividends if improved accuracies can be obtained by using shape functions other than polynomials. This is the case when the homogeneous solution of the pertinent differential equation is available for the development of each element matrix. For static analysis, use of the homogeneous solution of the differential equation yields the exact stiffness matrix and load vector for an element [17].

1.2. DYNAMIC STIFFNESS MATRIX (DSM) FORMULATION

For the dynamic analysis, a similar procedure, leading to only one matrix [called the Dynamic Stiffness Matrix (DSM)], which has both mass and stiffness properties, may be used. The DSM approach has been applied to the vibration analysis of rotating beams on different occasions [11–14], but the terminology DSM is much older [18–21]. In this case, the homogeneous solution, and hence also the dynamic stiffness matrix, become frequency dependent. Then, the resultant eigenvalue problem is written in the form

$$[K_{DS}(\omega)]\{w\} = \{0\} \tag{2}$$

which is no longer a linear relationship.

The DSM method has certain advantages over the conventional finite element method, particularly when higher frequencies and better accuracies of results are required. Often, the properties obtained from the DSM method are based on the closed form analytical solution of the differential equation of the element and hence are justifiably called "exact", if the differential equation can be solved exactly [22]. However, "exact" equations exist for important structures, such as plane frames, grids, and many plate and shell problems, which incorporate dynamic functions. The exact member equations DSM are then used to assemble the overall DSM, K_{DS}, of the structure. The elements of K_{DS} are thence transcendental functions of circular frequency. Hence, to solve the resultant eigenvalue problem (2), which is a non-linear one, appropriate algorithms have to be used.

A method based on the Sturm sequence root counting technique was first presented by Wittrick and Williams [20] to find the natural frequencies of elastic structures. This method has been developed previously, in specific contexts of prismatic plate assemblies [21] and plane frames [19]. Subsequently it was demonstrated as a unified method for buckling and vibration problems. The method has been used and adapted extensively, to cover numerous specific problems. For the axially loaded Timoshenko members, considering a uniform distribution of the mass, the exact DSM is presented by Howson and Williams [11] in which the effect of axial load, rotary inertia and shear deflection may be accounted for.

A theorem was presented by Wittrick and Williams [12] which can be used for the systematic calculation of the natural frequencies of either a discrete system which is assembled from sub-structures, or an assembly of distributed mass members. The application of the theorem to a spinning two-dimensional frame, with distributed mass members, was discussed where the constituent members were considered to be straight, uniform Bernoulli–Euler beams. When the Timoshenko members are considered, the DSM presented by Howson and Williams [11] can be used as the principal block in the calculation of natural frequencies of spinning frames. An exact Bernoulli–Euler DSM for a range of tapered beams, was presented by Banerjee and Williams [23], and Banerjee and Fisher [22] presented the coupled bending-torsional DSM for axially loaded beam elements. Reference [24] presented a very good and complete literature survey of numerous problems treated by the DSM method.

However, in all of these cases, the governing differential equations can be solved exactly. But it implies, sometimes, mathematical procedures which are difficult to deal with, and/or are limited to special cases (as in the case of Banerjee and Williams [23] for a range of tapered beams, where the Bessel functions are used).

In a large number of vibration problems, the pertinent governing differential equations have variable coefficients which makes it impossible to solve them exactly. Hence, some simplifying assumptions have to be considered to change the governing differential equations by introducing constant coefficients. For example, let us consider a spinning two-dimensional frame, with distributed mass members, where the constituent members were considered to be straight, uniform, Bernoulli–Euler beams. In such a case, an expedient way of dealing with a member with varying axial force (T) would be to break it down into several members, joined end to end, with such length that they can all presumably have constant force T [12]. Reference [13], presenting a general computational technique for the accurate analysis of forced vibration of rotating linear structures, follows also the same principle. Within each beam element, in that case, the axial force is taken as constant and equal to the mean value of the true centrifugal sectional force in that element. Then assembling the DSMs, obtained by "exact" member equations, the overall stiffness matrix is found.

1.3. DYNAMIC FINITE ELEMENTS (DFE) METHOD

Let us consider a tapered beam, rotating at a constant angular velocity about an axis at one end, and vibrating laterally. The variable coefficients, in this case,

are due to the non-uniform geometry and the centrifugal force which varies along the beam. To change the corresponding differential equations to those with constant coefficients, the beam will have to be broken down into members of unifom geometry and with such length that they can all presumably have constant force T. Then, as it will be seen later, when calculating the first natural frequencies for a specified precision, the DSM method takes approximately the same effort as in the FE method (see Figures 6–11). However, in this case, the DFE method can be advantageously exploited. The DFE method can be considered as a combination of two methods; the well known formulation procedure as in the FEM is adopted to provide a general tool, and the advantages of the DSM method are retained by choosing the weighting functions, shape functions, etc., referring to an appropriate exact member equation. The details of this procedure are described in the theory. A similar approach has been already applied by the authors, to the vibrational analysis of linearly tapered beams [25] and that of rotating uniform beams [26] and that of spinning linearly tapered beams [27].

An Euler–Bernoulli beam rotating about a fixed axis in space undergoing bending motion in a plane fixed in a reference system rotating with the beam is considered. The plane, in which the beam is bending, makes an angle θ with the rotating vector. The development of the DFE for lateral free vibration of a rotating beam is presented. Then, the method of incorporating the derived element matrices in a computer program is discussed with a particular reference to the established Williams–Wittrick algorithm. The application of the theory is demonstrated by the results obtained for a variety of configurations of rotating cantilever beams. As the elementary Bernoulli–Euler beam theory is used, the derivation assumes that rotary inertia and shear deflection are neglected.

2. MATHEMATICAL MODEL

Let us consider an Euler–Bernoulli beam rotating in space and undergoing bending motion in a plane fixed in a reference system rotating with the beam (Figure 1). The beam is assumed to be inextensible and the shear and mass axes are assumed to be coincident. The plane in which the beam undergoes pure bending makes an angle θ with the rotating vector. For $\theta = 0$, the motion is purely out-of-plane (flapping); for $\theta = \pi/2$ the motion is purely in-plane (lead-lag).

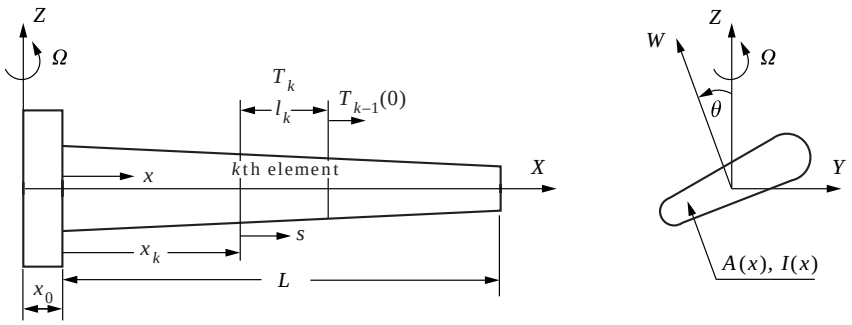

Figure 1. Geometry of rotating beam.

Figure 2. Domain discretized by a number of 2-node elements.

According to D'Alembert's principle, the total force per unit volume acting on the beam in the w direction is given by Hoa [9]:

$$F_2 = \rho(w_{,tt} - \Omega^2 \sin^2\theta w). \tag{3}$$

The corresponding differential equation of motion (for the centrifugally stiffened beam) is written as

$$[H_{fy}(x)w_{,xx} - [T(x)w_{,x}]_{,x} + m(x)(w_{,tt} - \Omega^2 \sin^2\theta w) = 0, \tag{4}$$

and

$$\frac{\mathrm{d}T}{\mathrm{d}x} + \Omega^2 m(x)(x_0 + x) = 0 \quad \text{or} \quad T(x) = \Omega^2 \int_x^L m(s)(x_0 + s)\,\mathrm{d}s. \tag{5}$$

Appropriate boundary conditions are imposed at $x = 0, L$. For example:

$$\text{Clamped:} \quad x = 0; \qquad w = w' = 0,$$

$$\text{Free:} \quad x = L; \qquad w'' = 0; \qquad [H_{fy}(x)w_{,xx}]_{,x} - T(x)w_{,x} = 0, \text{ etc.}$$

Equation (5) represents the centrifugal force acting along the beam, and x_0 represents the offset (the radius of the rotor on which the beam is mounted). For a vibration problem we suppose

$$w(x, t) = w(x)\exp(\mathrm{i}\omega t), \tag{6}$$

where ω represents the natural vibration frequencies. Substituting equation (6) into equation (4) we obtain

$$[H_{fy}(x)w_{,xx}]_{,xx} - [T(x)w_{,x}]_{,x} - m(x)\omega^2 w - m(x)\Omega^2 \sin^2\theta w = 0. \tag{7}$$

The Galerkin type weak form associated to equations (4) is

$$\mathscr{W} = \int_0^L \{H_{fy}(x)\delta w_{,xx}w_{,xx} + T(x)\delta w_{,x}w_{,x} - m(x)\omega^2\delta w w - m(x)\Omega^2 \sin^2\theta\delta w w\}\,\mathrm{d}x$$

$$+ [H_{fy}(x)(\delta w w_{,xxx} - \delta w_{,x}w_{,xx}) - T(x)\delta w w_{,x}]_0^L = 0. \tag{8}$$

For clamped-free boundary conditions: $\delta w = \delta w' = 0$ at $x = 0$, and force terms are zero at $x = L$. Here, w is a solution function and δw is a test function. Both quantities are defined in the same approximation space.

If the domain is discretized by a number of 2-node elements [28], we have (see Figure 2)

$$\mathscr{W} = \mathscr{W}_{INT} - \mathscr{W}_{EXT} = \sum_{k=1}^{NE} \mathscr{W}^k - \mathscr{W}_{EXT} = 0, \tag{9}$$

where

$$\mathscr{W}^k = \int_{x_j}^{x_{j+1}} \{H_{fy}(x)\delta w_{,xx} w_{,xx} + T(x)_k \delta w_{,x} w_{,x} - m(x)\omega^2 \delta w w$$

$$- m(x)\Omega^2 \sin^2\theta \delta w w\} \, \mathrm{d}x. \tag{10}$$

Each element is defined by nodes j, $j+1$ with corresponding coordinates and the centrifugal force, for element k, is defined as

$$T_k(x) = \Omega^2 \int_x^{l_k} m(x)(x_0 + x) \, \mathrm{d}x + T_{k-1}(0). \tag{11}$$

The relation $\mathscr{W}^k$ may also be written in an equivalent form obtained after two integration by parts on each element:

$$\mathscr{W}^k = \int_{x_j}^{x_{j+1}} w\{(H_{fy}(x)\delta w_{,xx})_{,xx} - (T(x)_k \delta w_{,x})_{,x} - m(x)\omega^2 \delta w$$

$$- m(x)\Omega^2 \sin^2\theta \delta w\} \, \mathrm{d}x + [\delta w_{,xx} H_{fy}(x) w_{,x}$$

$$- (\delta w_{,xxx} H_{fy}(x) - T(x)_k \delta w_{,x}) w]_{x_j}^{x_{j+1}}. \tag{12}$$

The admissibility condition for finite element approximation is controlled by equations (8). The approximation for w, δw is of e^1-type, assuring continuity of w and $w_{,x}$ at each node. Equation (12) presents simply another way of evaluating equations (11) at the element level.

2.1. FINITE ELEMENT METHOD (FEM) APPROACH

The classical Finite Element (FE) model is found by using Hermite type polynomial approximation as

$$w(x) = N_1(x)w_1 + N_2(x)w_{1,x} + N_3(x)w_2 + N_4(x)w_{2,x} \tag{13}$$

where w_1 and w_2 are nodal values at node j, $j+1$, corresponding to flexural displacements. Identical approximation is chosen for δw. The discretized representation of equation (8) is then obtained as:

$$\sum_{k=1}^{NE} \mathscr{W}^k = \mathscr{W}_{EXT}$$

which for the free vibration leads to:

$$[K]\{w_n\} - \lambda[M]\{w_n\} = \{0\}. \tag{14}$$

This is a classical linear eigenvalue problem which is solved using an inverse iteration, subspace or Lanczos method [16].

2.2. DYNAMIC STIFFNESS MODEL (DSM)

In some cases, one can obtain the DSM model in a manner different from the usual approaches. In fact, there is a possibility of obtaining the same DSM model by following the finite element formulation pattern, if approximation space is defined by frequency dependent hyperbolic functions.

Let us consider the case for which all parameters are constant over the element space: $H_{fy}(x)$, $T(x)$, $m(x)$, etc. One can then choose the interpolation functions $N_i(x, \hat{\omega})$ which are solutions of integral terms of equation (12):

$$H_{fy}\delta w_{,xxxx} - T\delta w_{,xx} - a^2\delta w = 0 \tag{15}$$

or

$$H_{fy}N_{i,xxxx} - TN_{i,xx} - a^2N_i = 0, \tag{16}$$

where

$$a^2 = m(x)(\underbrace{\omega^2 + \Omega^2 \sin^2\theta}_{\hat{\omega}^2}) \tag{17}$$

and N_i respect the nodal properties: e.g., $N_1 = 1, N_{1,x} = 0$ at $x = x_j$; $N_1 = 0, N_{1,x} = 0$ at $x = x_{j+1}$; etc.

Equation (12) can also be rewritten in the following non-dimensionalized form which is simply another way of evaluating this equation at the "reference element" level (Figure 3):

$$W^k_{ND} = \int_0^1 \left(\frac{\gamma_k}{\bar{l}_k^3}\,\delta w'''' - \left(\frac{\tau_k}{\bar{l}_k}\,\lambda^2\right)\delta w'' - \mu^2\bar{m}_k\bar{l}_k\delta w\right)w\,\mathrm{d}\xi$$

$$+\frac{\gamma_k}{\bar{l}_k^3}\,[\delta w''w' - \delta w'''w]_0^1 + \frac{\tau_k}{\bar{l}_k}\,\lambda^2[\delta w'w]_0^1, \tag{18}$$

where prime ($'$) denotes differentiation with respect to ξ.

The interpolation functions, in this case, are obtained as follows.

First, using generalized parameters, the solution function w, and the test function δw, are written as

$$\delta w(\xi) = \langle P(\xi)\rangle * \{\delta a\}, \qquad w(\xi) = \langle P(\xi)\rangle * \{a\}, \tag{19}$$

Figure 3. A 2-node reference beam element of four degrees of freedom.

where the basis functions of the approximation are

$$\langle P(\xi)\rangle = \left\langle \cos(\alpha\xi); \frac{\sin(\alpha\xi)}{\alpha}; \frac{\cosh(\beta\xi) - \cos(\alpha\xi)}{\alpha^2 + \beta^2}; \frac{\sinh(\beta\xi) - \sin(\alpha\xi)}{\alpha^3 + \beta^3} \right\rangle \quad (20)$$

which are solutions of integral terms of equation (18), and, in addition, they are chosen in a such manner to lead to classical basis functions of the standard "Hermite" beam element as α, and $\beta \to 0$. Here,

$$\alpha, \beta = \frac{1}{[2 * A]^{1/2}} \{-B \pm [B^2 - 4A * C]^{1/2}\}^{1/2}, \quad (21)$$

where

$$A = \frac{\gamma_k}{\bar{l}_k}, \qquad B = -\left(\frac{\tau_k}{\bar{l}_k}\lambda^2\right), \qquad C = -\mu^2 \bar{m}_k \bar{l}_k.$$

Note that the generalized parameters of the approximation have, in general, no direct physical meaning. Thus, $\langle \delta a \rangle$ and $\langle a \rangle$ are more conveniently replaced by nodal variables $\langle \delta w_1; \delta w_1'; \delta w_2; \delta w_2' \rangle$, and $\langle w_1; w_1'; w_2; w_2' \rangle$, respectively. To this end, regarding equation (19), one can write:

$$\{\delta w_n\} = [P_n] * \{\delta a\}, \qquad \{w_n\} = [P_n] * \{a\}, \quad (22)$$

where

$$[P_n] = \begin{bmatrix} 1 & 0 & 0 & 0 \\ 0 & 1 & 0 & \dfrac{(\beta - \alpha)}{(\alpha^3 + \beta^3)} \\ \cos(\alpha) & \dfrac{\sin(\alpha)}{\alpha} & \dfrac{[\cosh(\beta) - \cos(\alpha)]}{(\alpha^2 + \beta^2)} & \dfrac{\sinh(\beta) - \sin(\alpha)]}{(\alpha^3 + \beta^3)} \\ -\alpha \sin(\alpha) & \cos(\alpha) & \dfrac{[\beta \sinh(\beta) + \alpha \sin(\alpha)]}{(\alpha^2 + \beta^2)} & \dfrac{[\beta \cosh(\beta) - \alpha \cos(\alpha)]}{(\alpha^3 + \beta^3)} \end{bmatrix}. \quad (23)$$

Then, from equations (19), (22) and (23) the approximations in nodal variables can be written as

$$\delta w(\xi) = \langle P(\xi)\rangle [P_n]^{-1} \{\delta w_n\} = \langle N(\xi)\rangle \{\delta w_n\},$$
$$w(\xi) = \langle P(\xi)\rangle [P_n]^{-1} \{w_n\} = \langle N(\xi)\rangle \{w_n\}, \quad (24)$$

where

$$\langle N\rangle = \langle N_1(\xi, \hat{\omega});\quad N_2(\xi, \hat{\omega});\quad N_3(\xi, \hat{\omega});\quad N_4(\xi, \hat{\omega})\rangle$$

represent the frequency dependent dynamic shape functions, mentioned earlier.

Equations (24) represent simply another way of writing equations (19) in nodal form. It can be easily shown that the dynamic shape functions $\langle N\rangle$ also satisfy the integral terms of equation (18). They are found to be

$$\begin{aligned}
N_1(\xi, \hat{\omega}) = {} & \frac{(\alpha\beta)}{D} * \{-\cos(\alpha\xi) \\
& + \cos(\alpha(1-\xi)) * \cosh(\beta) + \cos(\alpha) * \cosh(\beta(1-\xi)) \\
& - \cosh(\beta\xi) - \frac{\beta}{\alpha} * \sin(\alpha(1-\xi)) * \sinh(\beta) \\
& + \frac{\alpha}{\beta} * \sin(\alpha) * \sinh(\beta(1-\xi))\},
\end{aligned}$$

$$\begin{aligned}
N_2(\xi, \hat{\omega}) = {} & \frac{1}{D} * \{\beta * [\cosh(\beta(1-\xi)) * \sin(\alpha) \\
& - \cosh(\beta) * \sin(\alpha(1-\xi)) - \sin(\alpha\xi)] \\
& + \alpha * [\cos(\alpha(1-\xi)) * \sinh(\beta) \\
& - \cos(\alpha) * \sinh(\beta(1-\xi)) - \sinh(\beta\xi)]\},
\end{aligned}$$

$$\begin{aligned}
N_3(\xi, \hat{\omega}) = {} & \frac{(\alpha\beta)}{D} * \{-\cos(\alpha(1-\xi)) \\
& + \cos(\alpha\xi) * \cosh(\beta) - \cosh(\beta(1-\xi)) \\
& + \cos(\alpha) * \cosh(\beta\xi) - \frac{\beta}{\alpha} * \sin(\alpha\xi) * \sinh(\beta) \\
& + \frac{\alpha}{\beta} * \sin(\alpha) * \sinh(\xi)\},
\end{aligned}$$

$$\begin{aligned}
N_4(\xi, \hat{\omega}) = {} & \frac{1}{D} * \{\beta * [-\cosh(\beta\xi) * \sin(\alpha) \\
& + \sin(\alpha(1-\xi)) + \cosh(\beta) * \sin(\alpha\xi) \\
& - \alpha * [\cos(\alpha\xi) * \sinh(\beta) \\
& + \sinh(\beta(1-\xi)) + \cos(\alpha) * \sinh(\beta\xi)]\}
\end{aligned}$$

and

$$D = (\alpha\beta) * \{-2 * (1 - \cos(\alpha) * \cosh(\beta)) + \left(\frac{\alpha^2 - \beta^2}{\alpha\beta}\right) * \sin(\alpha) * \sinh(\beta)\}. \qquad (25)$$

Using expressions (25) the discretized approximation of equation (18) is obtained as

$$W_{ND}^{k} = \langle \delta w_n \rangle [K_{DS}]^k * \{w_n\}, \tag{26}$$

where the dynamic stiffness matrix is now

$$[K_{DS}]^k = \frac{\gamma_k}{l_k^3} [\{N'''\}_0 \{-N''\}_0 \{-N'''\}_1 \{N''\}_1]$$

$$+ \left(\frac{\tau_k}{l_k} \lambda^2 \right) [\{-N'\}_0 \{0\} \{N'\}_1 \{0\}]. \tag{27}$$

The assembled model of equation (8) is then obtained as

$$\mathscr{W} = \sum_{k=1}^{NE} \mathscr{W}^k = [K_{DS}(\hat{\omega})]\{w_n\} = 0. \tag{28}$$

This is a non-linear eigenvalue problem which is solved using a bisection method proposed by Wittrick and Williams described on several occasions in the literature [19, 20, 29, 30].

The stiffness matrix found by this approach is based on the closed form analytical solution of the differential equation of the element and hence, gives justifiably the "exact" results. This stiffness matrix is found to be identical to the "exact Dynamic Stiffness Matrix (DSM)" presented by Howson and Williams [11].

The frequency dependent dynamic shape functions of equations (25) corresponding to a rotating uniform beam element, are shown in Figure 4. The effect of frequency changes on the form of these shape functions is demonstrated in these figures. The rotating speed is assumed to be the same for all cases ($\Omega = 12$ rad/s). In addition, the effect of the spinning speed on the form of the dynamic shape functions was studied. As it can be observed in Figure 5, when the rotating velocity of the beam increases, the shape functions' amplitude decreases. (The fourth dynamic shape function of the same uniform beam element as in Figure 4 is presented here.) It can be explained by the stiffening effect of the centrifugal force due to the spinning speed.

2.3. DYNAMIC FINITE ELEMENT (DFE) METHOD

When coefficients $H_{fy}(x)$, $T(x)$, $m(x)$, etc. are not constant, it becomes difficult and cumbersome or even impossible to obtain the exact model as presented in the preceding section. The approximation space, in this case, depends on the nature of the space variation of these parameters. In this study we propose an intermediate approach, where the interpolation functions are obtained with averaged value parameters over each element. The influence of the parameter

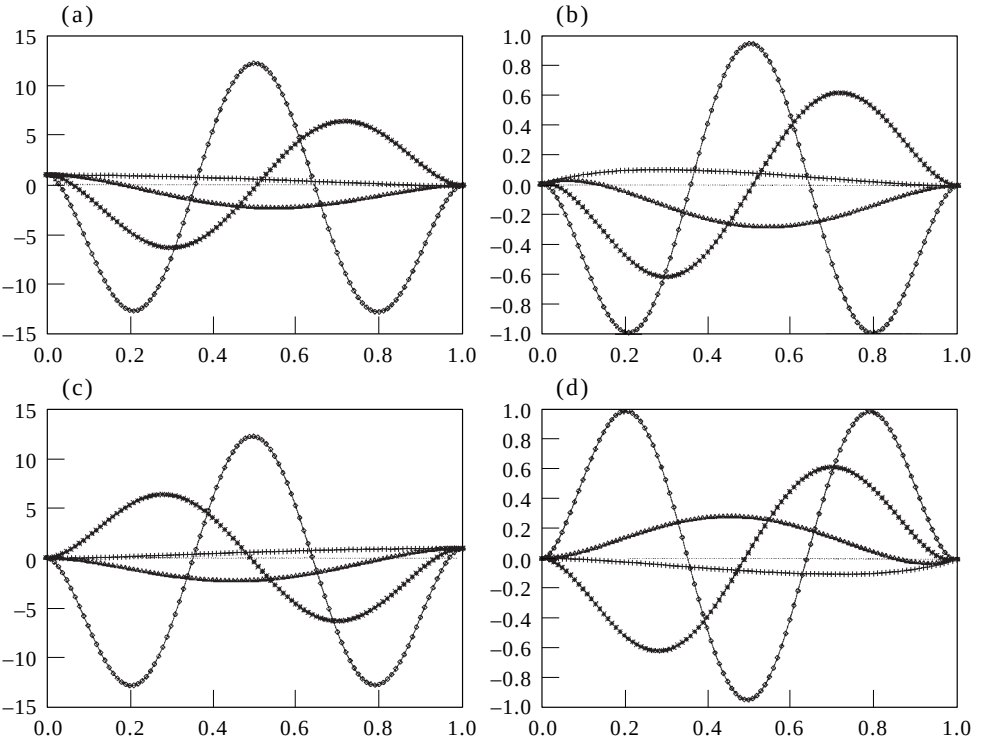

Figure 4. The variation of the dynamic shape functions N_i vs frequency changes for a rotating uniform beam; $E = 1$ GPa, $A = 1$ m^2, $L = 1$ m, $\rho = 1$ kg/m^3, $I = 1$ m^4, $\Omega = 12$ rad/s. (a) N_1; (b) N_2; (c) N_3; (d) N_4; —×—, ω_1, 1st natural frequency; —△—, ω_2, 2nd natural frequency; —∗—, ω_3, 3rd natural frequency; —◇—, ω_4, 4th natural frequency.

variation is taken into account by rewriting the virtual elementary work of equations (11) as

$$\mathscr{W}^k = \int_{x_j}^{x_{j+1}} \{H_{fy}\delta w_{,xx}w_{,xx} + T\delta w_{,x}w_{,x} - m\hat{\omega}^2\delta ww\}\,\mathrm{d}x$$

$$+ \int_{x_j}^{x_{j+1}} \{-\underbrace{(H_{fy} - H_{fy}(x))}_{H_{fyDEV}}\delta w_{,xx}w_{,xx} - \underbrace{(T - T(x))}_{T_{DEV}}\delta w_{,x}w_{,x}$$

$$+\underbrace{(m - m(x))}_{m_{DEV}}\hat{\omega}^2\delta ww\}\,\mathrm{d}x \tag{29}$$

which contains two parts: the first part is the same as the elementary virtual work associated to an assumed axially loaded uniform beam of constant parameters. The second part represents the influence due to the space variation of centrifugal force and geometrical parameters.

After two integration by parts, equation (29) can be written in the following non-dimensionalized form which is simply another way of evaluating this equation at the "reference" level:

$$W_{ND}^{k} = \int_0^1 \underbrace{\left(\frac{\gamma_k}{\bar{l}_k^3}\,\delta w'''' - \left(\frac{\tau_k}{\bar{l}_k}\,\lambda^2\right)\delta w'' - \mu^2 \bar{m}_k \bar{l}_k \delta w\right)}_{(*)} w \,\mathrm{d}\xi$$

$$+\frac{\gamma_k}{\bar{l}_k^3}\,[\delta w'' w' - \delta w''' w]_0^1 + \frac{\tau_k}{\bar{l}_k}\,\lambda^2[\delta w' w]_0^1 + DEV., \tag{30}$$

where

$$DEV. = -\left(\frac{1}{\bar{l}_k^3}\right)\int_0^1 (\gamma_{DEV} w'' \delta w'')\, d\xi$$

$$-\left(\frac{\lambda^2}{\bar{l}_k}\right)\int_0^1 (\tau_{DEV}\omega' \delta w')\,\mathrm{d}\xi$$

$$+(\mu^2 \bar{l}_k)\int_0^1 (\bar{m}_{DEV} w \delta w)\,\mathrm{d}\xi. \tag{31}$$

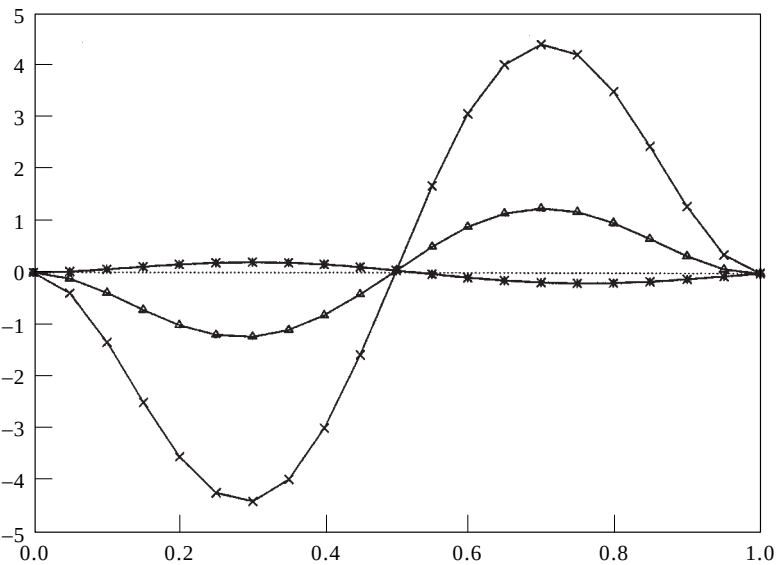

Figure 5. The change of the fourth dynamic shape function, N_4, at the third natural frequency, ω_3, vs spinning speed (the same rotating uniform beam as in Figures 4 in considered). —×—, $\Omega = 4$ rad/s; —△—, $\Omega = 8$ rad/s; —∗—, $\Omega = 12$ rad/s.

Then, the approximation functions found in the preceding section are used which make the expression (*) become zero, and the finite element model leads to

$$W_{ND}^{k} = \langle \delta w_n \rangle [K_{DS}]^{k} * \{w_n\}, \tag{32}$$

where

$$[K_{DS}]^{k} = [K_{DS}]_{Average}^{k} + [K_{DS}]_{DEV}^{k} \tag{33}$$

and

$$[K_{DS}]_{Average}^{k} = \frac{\gamma_k}{\bar{l}_k} [\{N'''\}_0\{-N''\}_0\{-N'''\}_1\{N''\}_1]$$

$$+ \left(\frac{\tau_k}{\bar{l}_k}\lambda^2\right)[\{-N'\}_0\{0\}\{N'\}_1\{0\}], \tag{34}$$

$$(K_{DSij})_{DEV}^{k} = -\left(\frac{1}{\bar{l}_k}\right)\int_0^1 \gamma_{DEV.} N_i'' N_j''\, \mathrm{d}\xi$$

$$-\left(\frac{\lambda^2}{\bar{l}_k}\right)\int_0^1 \tau_{DEV}.N_i' N_j'\, \mathrm{d}\xi$$

$$+ (\mu^2 \bar{l}_k)\int_0^1 \bar{m}_{DEV}.N_i N_j\, \mathrm{d}\xi. \tag{35}$$

It can be readily verified from equations (27) and (34) that the second terms in both equations reduce to zero when $\lambda = 0$, i.e., when the beam does not rotate. Thus, the degenerated stiffness matrix of equation (34) becomes that of a non-uniform Bernoulli–Euler beam [25], whereas equation (27) changes to the stiffness matrix corresponding to a uniform Bernoulli–Euler beam presented on several occasions in the literature [19, 20, 30]. Neglecting the deviatoric terms due to the geometric parameters, but retaining $\lambda > 0$, the stiffness matrix of equation (34) becomes that of centrifugally stiffened uniform beams [26]. Further more, the resultant stiffness matrix will be similar to the case presented by Howson and Williams [11], if all of the deviatoric terms are neglected.

It can be also verified that when $\omega \to 0$, for the case of non-rotating beams, the functions of expression (20) become $1; x; x^2; x^3$, respectively, which are the expansion terms in the formulation of the "Hermite" beam element, in conventional finite element method. In this case, the shape functions of equations (25) become the corresponding shape functions, and therefore, the dynamic stiffness matrix of equations (27) and (34) change to a static stiffness matrix of a "Hermite" beam element [28].

3. APPLICATION OF THE THEORY

The expressions for the DFE stiffness matrix derived in the previous sections can be directly exploited to compute the natural frequencies of centrifugally stiffened beams. Elementary matrices will have to be assembled in the usual way to form the overall dynamic stiffness matrix $[K_{DS}]$ of the final structure. The determination of the natural frequency then follows from the assembled dynamic stiffness matrix $[K_{DS}]$ and the well-known Wittrick–Williams algorithm described on several occasions in the literature [19, 20, 29, 30].

Suppose that ω denotes the circular frequency of the beam. Then it is known that the number of natural frequencies, j, lying between $\omega = 0$ and $\omega = \omega^*$ is given by [20]

$$j = j_0 + s\{K_{DS}\}, \tag{36}$$

where $[K_{DS}]$ is the overall dynamic stiffness matrix (which is ω dependent) of the structure, evaluated at $\omega = \omega^*$; $s\{K_{DS}\}$ is the number of negative elements on the leading diagonal of $K_{DS}^{\triangle}$; $K_{DS}^{\triangle}$ is the upper triangular matrix obtained by applying the usual form of Gauss elimination to K_{DS} and j_0 is the number of natural frequencies of the beam still lying between $\omega = 0$ and $\omega = \omega^*$ when the displacement components to which K_{DS} corresponds are all zero (the beam can still have natural frequencies when all its nodes are clamped, because the presented formulation allows each individual element to have an infinite number of degrees of freedom between nodes). Thus

$$j_0 = \sum_{m=1}^{EN} j_m, \tag{37}$$

where j_m is the number of natural frequencies between $\omega = 0$ and $\omega = \omega^*$ for an element with its ends clamped, while the summation extends over all elements. For the element stiffness matrix developed in this paper, the clamped-clamped frequencies of an individual element occur when one or more of the components of the matrices of equations (34) and (35) become infinite, and this will occur when $D = 0$, where D is the denominator expression in equation (25) and it is exactly the same equation as the case of a clamped–clamped axially loaded uniform beam element. Clearly, it is a difficult task to find the component of j_m arising from equation (25). However, since these roots are the natural frequencies of the beam which involve bending they can be easily obtained as described here. Consider a simply supported beam with moments applied at its ends. With this simply supported beam treated as a complete structure, for which the stiffness matrix is B, it is shown by Howson and Williams [11] that

$$j_m = j_c - s\{B\}, \tag{38}$$

where j_c is the number of natural frequencies of the simply supported beam exceeded by ω^*. Thus, exploiting the relations in equations (36–38), it is possible to converge on any required natural frequency given the fact that the expressions for the DFE stiffness matrix and the clamped-clamped natural frequencies are

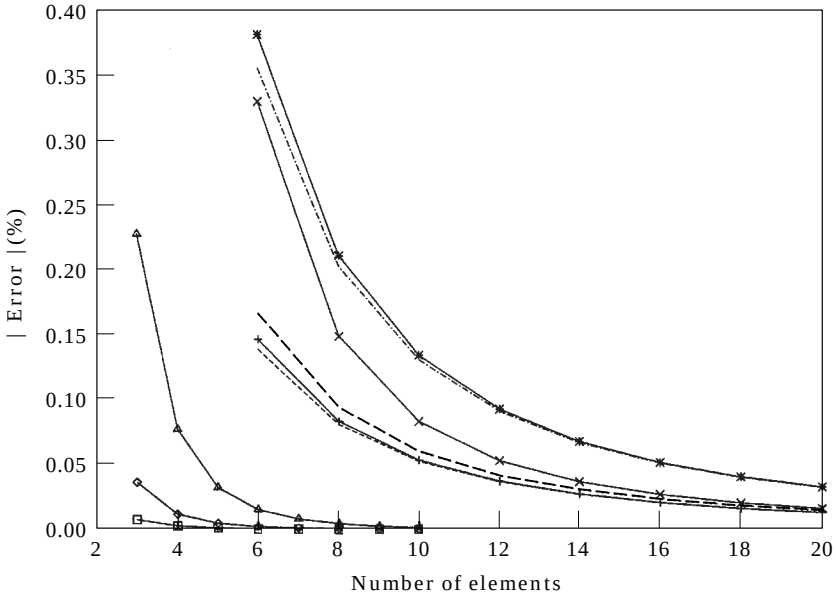

Figure 6. Convergency test, resulting from three different methods, for a cantilever uniform beam; the first three natural frequencies (μ_i) of the flapping vibrations ($\theta = 0$) for a constant spinning speed ($\lambda = 6$) is considered; —+—, μ_1 by FE; ----, μ_1 by DSM; —◇—, μ_1 by DFE; —∗—, μ_2 by FE; –·–·–, μ_2 by DSM; —△—, μ_2 by DFE; —×—, μ_3 by FE; ———, μ_3 by DSM; —□—, μ_3 by DFE.

known. Then, the mode shapes are calculated by using equation (2). The procedure explained here is implemented in a conventional finite element computer program called RE_FLEX [31] to obtain the results given in the next section.

4. NUMERICAL RESULTS

Some examples of the formulation presented in this paper are treated in this section. The following parameters were utilized in all of the examples of uniform beams: $E = 200$ GPa, $\rho = 1000$ kg/m^3, cross-sectional area $= 0{\cdot}012$ m^2, second moment of area $(I) = 0{\cdot}00001$ m^4, and the beam length is assumed to be $(L) = 1$ m.

4.1. VIBRATION OF A ROTATING UNIFORM BEAM FOR $\theta = 0$

Based on the theory presented in this paper, non-dimensional numerical results were obtained for the case of a cantilever uniform beam rotating at different speeds, and undergoing the out-of-plane (flapping) vibrations. The convergency rates for the first three non-dimensionalized natural frequencies (μ_i) as a function of the number of equal length elements and for $\lambda = 6$ are shown in Figure 6. The comparison were made between the results obtained by the presented DFE method, exact DSM method and those found by the conventional FEM, where the natural frequencies obtained by using 200 uniform classical "Hermite" finite beam elements were taken as reference values. Excellent agreements were found between these values and similar published results in reference [8], which justifies the use of these results as exact values.

In the FE model, the centrifugal force due to the rotating speed, is modelled as a preload by introducing the appropriate geometric stiffness matrix (see, for example, references [18] and [16]). The results due to the DSM method, in this case, are found by using the exact element of reference [11], when the rotary inertia and shear deformation are neglected. The axial force in both of the DSM and the conventional FEM models, is considered to be constant per element and it is assumed to be equal to the average value of the centrifugal force along each element.

As is can be observed, both of the classical FE and exact DSM methods lead to approximately the same convergency rates (the results, for the first and the third natural frequencies, are coincident; for the second one, the DSM method leads to a convergency rate which, for small number of elements, seems to be higher than the FEM, but when the number of elements is increased, both of them lead to similar results). As illustrated in Figure 6, much better convergency rates are found by the presented DFE method. Hence, for the rest of the following tests described in this section, further comparisons with the DSM method will be omitted.

In Figure 7, are shown the convergency rates for the first non-dimensionalized natural frequency (μ_1) as a function of the number of equal length elements, incorporating different rotating speeds ($\lambda = 1$, $\lambda = 6$ and $\lambda = 12$, respectively). Results similar to the preceding test were found.

The effect of eccentricity on the eigenfrequencies can also be considered. The stiffness characteristics of a rotating beam may also be modified by increasing the steady state internal preload due to the offset (the radius of the rigid rotating base on which the beam is mounted). The DFE method is exploited in the case of the

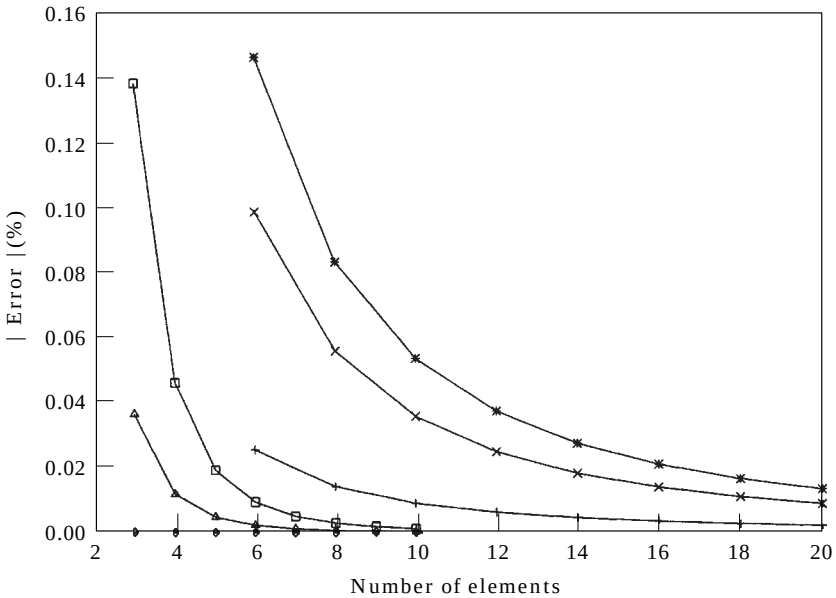

Figure 7. Convergency test, resulting from the classical and Dynamic finite element methods, for a cantilever uniform beam; the first natural frequency (μ_1) of the flapping vibrations ($\theta = 0$) for different spinning speeds; —+—, FE for $\lambda = 1$; —◇—, DFE for $\lambda = 1$; —∗—, FE for $\lambda = 6$; —△—, DFE for $\lambda = 6$; —×—, FE for $\lambda = 12$; —□—, DFE for $\lambda = 12$.

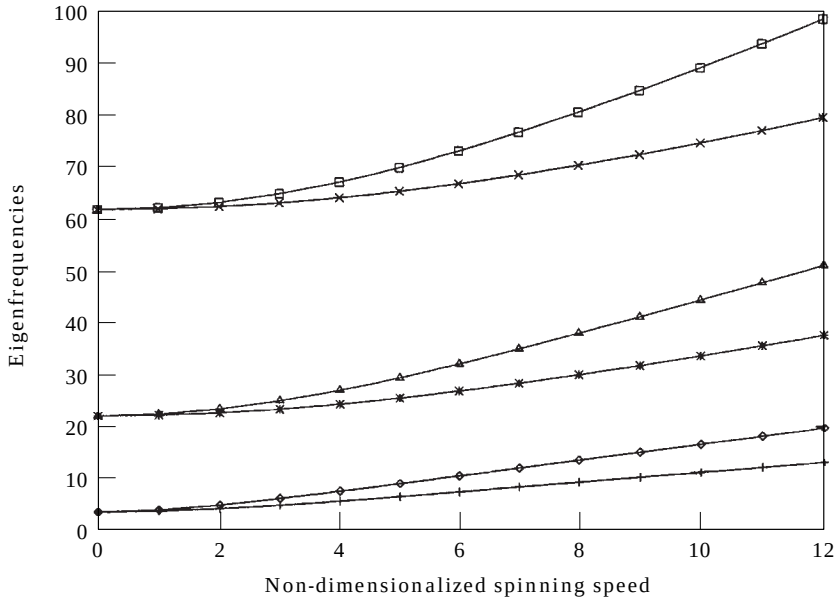

Figure 8. The effect of eccentricity (offset radius) on the first three natural frequencies of the out-of-plane vibrations of the cantilever uniform beam. —+—, 1st mode for $X_0=0$; —◇—, 1st mode for $X_0=1$; —★—, 2nd mode for $X_0=0$; —△—, 2nd mode for $X_0=1$; —×—, 3rd mode for $X_0=0$; —□—, 3rd mode for $X_0=1$.

uniform beam with an offset radiu $x_0 = 1$ m. The results obtained for the first three eigenfrequencies for $x_0 = 0$ and $x_0 = 1$ are shown in Figure 8, where the stiffening effect of the eccentricity is well illustrated.

4.2. VIBRATION OF A ROTATING UNIFORM BEAM FOR $\theta = \pi/2$

Let us consider the case of the in-plane (lead-lag) vibration of a uniform cantilever beam rotating at a constant angular velocity. The same parameters as in the previous example are utilized, and the following simulations are performed. First, the effect of centripetal acceleration [4] on the eigenfrequencies of the beam is studied. The comparisons were made between the results obtained by taking into account the centripetal acceleration term and those obtained when just the preload (centrifugal force) is considered. The corresponding results for the first natural frequency, obtained by the DFE method, are shown in Figure 9. Including the preload effects due to the centrifugal force field results in the well known "stiffening" effect. Combining the contribution due to centripetal acceleration with the influence of the preload slightly counteracts the stiffening effects of the preload [4]. The trends given in Figure 9 may be explained with the equations of motion presented earlier. Then, the convergency rates for the first four non-dimensionalized natural frequencies (μ_i) as a function of the number of equal length elements and also for $\lambda = 6$ are shown in Figure 10. The comparison was made between the results obtained by the DFE method and those found by the conventional FEM. Once more, much better convergency rates were obtained by the DFE method.

4.3. OUT-OF-PLANE VIBRATION OF A ROTATING TAPERED BEAM

The most general form of this theory is applied to the case of a cantilever, linearly tapered beam rotating at different speeds. For a group of cross-sections [23, 27] the taper, in two directions along the axial length, can be presented as

$$h(x) = h_r\left(1 + c_1\frac{x}{L}\right)^n, \qquad b(x) = b_r\left(1 + c_2\frac{x}{L}\right)^m,$$

$$A(x) = A_r\left(1 + c_1\frac{x}{L}\right)^n\left(1 + c_2\frac{x}{L}\right)^m, \qquad I(x) = I_r\left(1 + c_2\frac{x}{L}\right)^m\left(1 + c_1\frac{x}{L}\right)^{n+2}.$$

where h, A, I are the width, thickness, cross-section area and second moment of area, respectively; c_1 and c_2 are constant which must be > -1 because otherwise the beam tapers to zero between its extremities; for the case of a linear taper, n and m are usually 0 or 1; and subscript r denotes a value which is chosen as a reference. The Young's modulus, E, and density, ρ, of the member are assumed to be constant, and the length of the member is L. Here, a rotating linearly tapered beam is considered, where the width is assumed to be constant ($m = 0$ (or $c_2 = 0$), $c_1 = -1/2$ and $n = 1$).

Figure 11 presents the comparison made between the convergency rates obtained by the "exact DSM method", the conventional FEM and the DFE

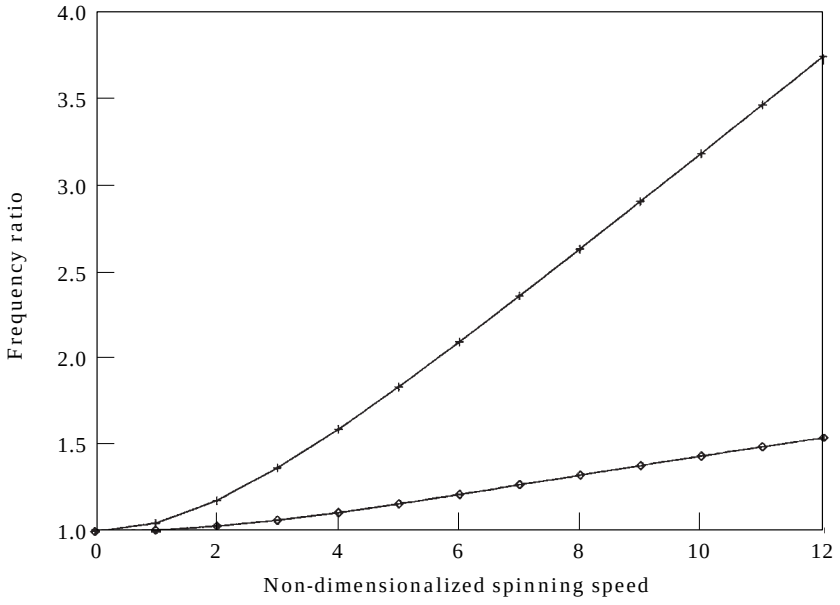

Figure 9. The effect of the centripetal acceleration on the first natural frequency of in-plane vibrations of the cantilever uniform beam. —+—, preload; —◇—, preload plus centripetal acceleration.

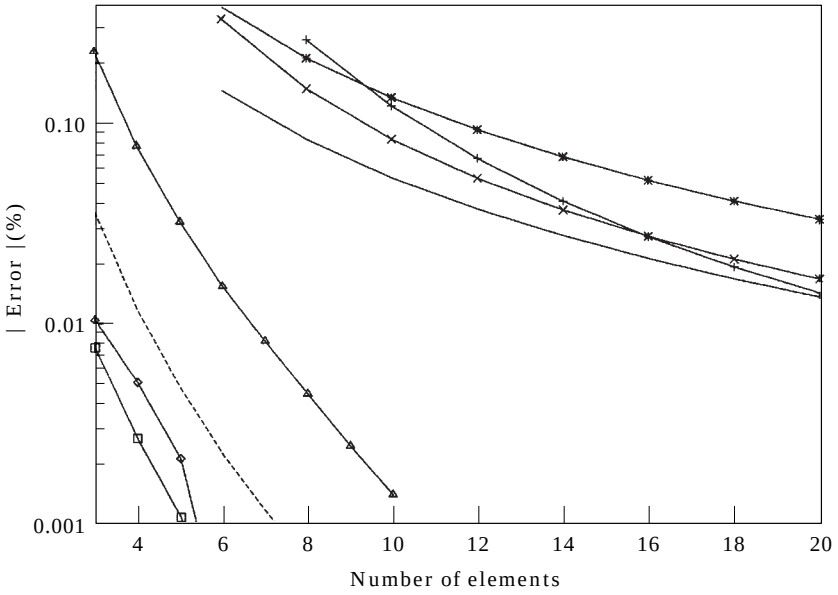

Figure 10. Convergency test for first four in-plane (lead-lag) natural frequencies ($\theta = \pi/2$) of a cantilever uniform beam and for $\lambda = 6$: ——, μ_1 by FE; ----, μ_1 by DFE; —★—, μ_2 by FE; —△—, μ_2 by DFE; —×—, μ_3 by FE; —□—, μ_3 by DFE; —+—, μ_4 by FE; —◇—, μ_4 by DFE.

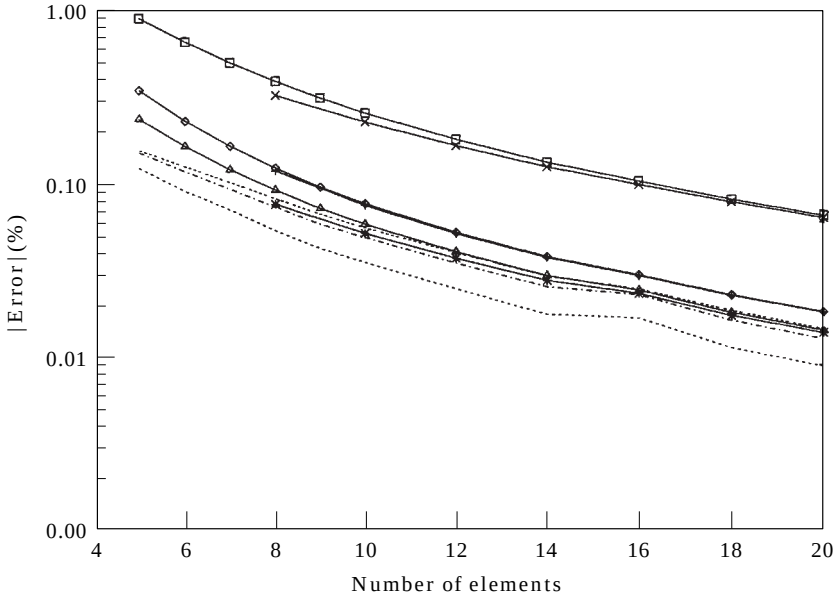

Figure 11. Comparison between the rates of convergence obtained by the DFE method and the corresponding results obtained by the conventional FE and the exact uniform DSM methods, for a rotating cantilever linearly tapered beam, $m = 0$, $n = 1$, $c_1 = -1/2$ and for $\lambda = 6$: —+—, μ_1 by FE; —◇—, μ_1 by DSM; ----, μ_1 by DFE; —★—, μ_2 by FE; —△—, μ_2 by DSM; ·-·-·-, μ_2 by DFE; —×—, μ_3 by FE; —□—, μ_3 by DSM; ——, μ_3 by DFE.

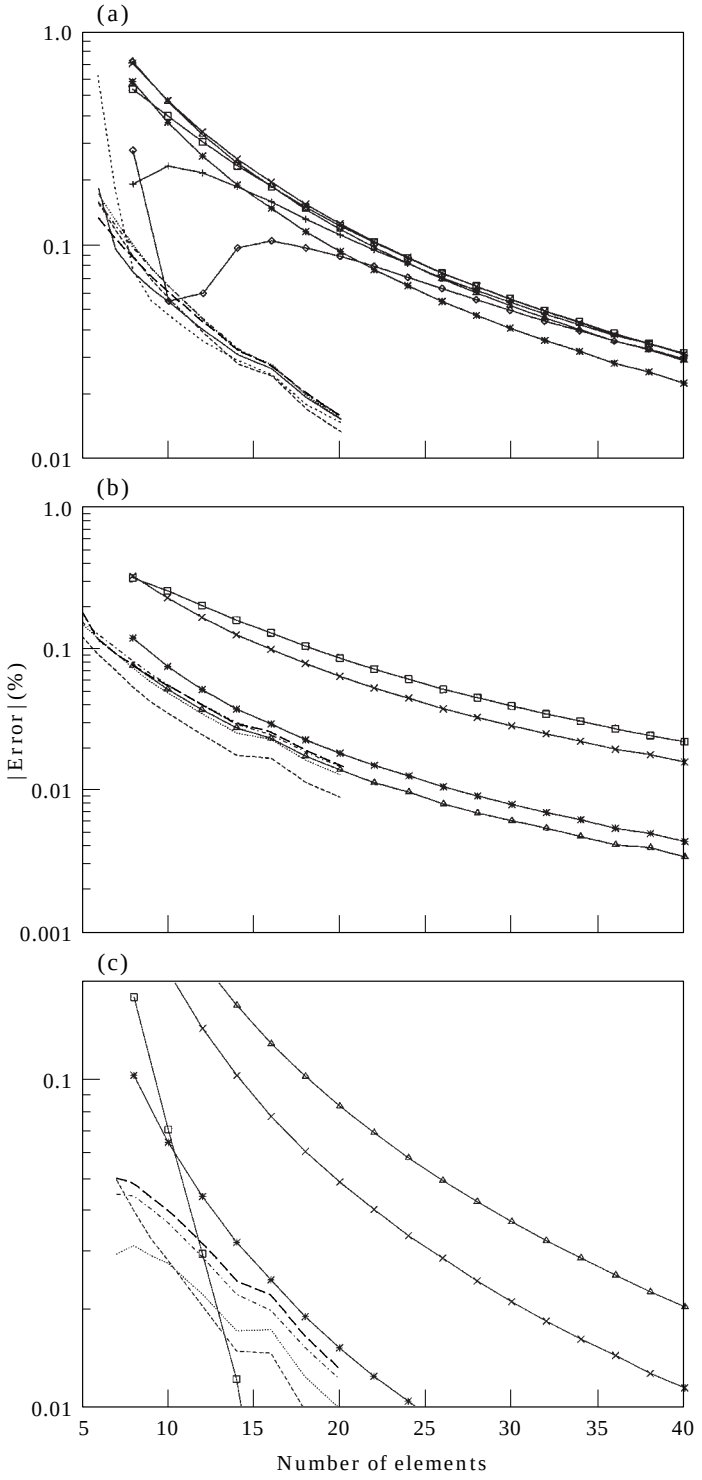

Figure 12. Comparison between the rates of convergence obtained by the DFE method and the corresponding results obtained by the conventional FE method, for a rotating cantilever linearly tapered beam; $m = 0$, $n = 1$, $c_1 = -1/2$ for $\lambda = 1$, $\lambda = 6$ and $\lambda = 12$. —★—, μ_1 by FE; ----, μ_1 by DFE; —△—, μ_2 by FE; · · · ·, μ_2 by DFE; —×—, μ_3 by FE; -·-·-·-, μ_3 by DFE; —□—, μ_4 by FE; —○—, μ_4 by DFE; —+—, μ_5 by FE; ——, μ_5 by DFE; —◇—, μ_6 by FE; ——, μ_6 by DFE.

method, for a constant rotating speed ($\lambda = 6$). The tapered cantilever beam, in this case, is discretized by "exact" uniform beam members and by uniform "Hermite" finite beam elements. The axial force in both of the DSM and the conventional FEM models, is considered to be constant per element and equal to the average value of the centrifugal force along each element. Where as in the DFE model, the variable centrifugal force is appropriately introduced.

The natural frequencies obtained by using 200 uniform classical "Hermite" finite beam elements, were taken as exact reference values, and the results are compared to them. Excellent agreements were, once more, found between these values and similar published results in reference [8], which justifies the use of these results as exact values. As it can be observed, for the first three natural frequencies, the same convergency rates, are obtained by the DSM approach and conventional FEM. As it is illustrated, for the first and third natural frequencies, much better convergency rates are found by the presented DFE method, where as for the second natural frequency, the difference between the presented method and two other methods, is less pronounced. Since both of the classical FE and exact DSM methods lead, generally, to approximately the same convergency rates, for the rest of the following tests due to the beams of tapered geometry, further comparisons with the DSM method was not necessary.

Figure 12(a), (b) and (c) show, respectively, the convergency rates for the first six and four natural frequencies (μ_i) as a function of the number of equal length elements, for different rotating speeds ($\lambda = 1$, $\lambda = 6$ and $\lambda = 12$; respectively). As it can be observed from the illustrated results, also for higher modes and spinning speeds, the DFE method, generally, lead to much better convergency rates. The same procedure can also be applied to analyze the lead-lag vibrations of the tapered beam.

5. CONCLUSION

A new DFE formulation to calculate the natural frequencies and mode shapes of Euler–Bernoulli rotating beams is presented. Explicit expressions for the frequency dependent trigonometric shape functions are derived. An expression for the natural frequencies of a member with constrained ends is also presented. Exploiting the developed model, together with an established algorithm [19], the lateral free vibration analysis of some configurations of uniform and linearly tapered rotating beams has been demonstrated. Numerical results, for various cases, showed approximately the same convergency rates for both "exact" DSM and FE models, where as, generally, much better results are found by the proposed method.

The DFE method can also be extended to more complex problems such as rotating beams with concentrated masses and the coupled vibration of beams and the assemblies made of beam elements.

On the other hand, it will be possible to take into account the effects of shear deformation and rotary inertia, which are significant for beams having large cross-sectional dimensions, in comparison to their length, and also when higher modes are important.

ACKNOWLEDGMENTS

The authors wish to acknowledge the scholarship awarded by the Ministry of Culture and Higher Education of Iran which made this work possible. The authors are also grateful to the Natural Sciences and Engineering Research Council of Canada which also supported this research.

REFERENCES

1. W. E. Boyce, R. C. Di Prima and G. H. Handelman 1954 *Proceedings of the Second National Congress of Applied Mechanics*, *Ann Arbor*, *Mich*., Vibrations of rotating beams of constant section; pp. 165–173.
2. W. F. Hunter 1970 NASA TN D-6064. Integrating matrix method for determining the natural vibration characteristics of propeller blades.
3. W. F. White Jr and R. E. Malatino 1975 NASA TM X-72, 751. A numerical method for determining the natural vibration characteristics of rotating nonuniform cantilever blades.
4. R. M. Laurenson 1976 *AIAA Journal* **14**(10), 1444–1450. Modal analysis of rotating flexible structures.
5. G. Surace, V. Anghel and C. Mares 1997 *Journal of Sound and Vibration* **206**(4), 473–486. Coupled bending–bending–torsion vibration analysis of rotating pretwisted blades: an integral formulation and numerical examples.
6. K. K. Gupta 1986 *International Journal for Numerical Methods in Engineering* **23**, 2347–2357. Formulation of numerical procedures for dynamic analysis of spinning structures.
7. K. K. Gupta and C. L. Lawson 1988 *International Journal for Numerical Methods in Engineering* **26**, 1029–1037. Development of block lanczos algorithm for free vibration analysis of spinning structures.
8. D. H. Hodges and M. J. Rutkowski 1981 *AIAA Journal* **19**(11), 1459–1466. Free-vibration analysis of rotating beams by a variable-order finite-element method.
9. S. V. Hoa 1979 *Journal of Sound and Vibration* **67**(3), 369–381. Vibration of a rotating beam with tip mass.
10. V. T. Nagaraj and P. Shanthakumar 1975 *Journal of Sound and Vibration* **43**(3), 575–577. Rotor blade vibrations by the Galerkin finite element method.
11. W. P. Howson and F. W. Williams 1973 *Journal of Sound and Vibration* **26**(4), 503–515. Natural frequencies of frames axially loaded Timoshenko members.
12. W. H. Wittrick and F. W. Williams 1982 *Journal of Sound and Vibration* **82**(1), 1–15. On the free vibration analysis of spinning structures by using discrete or distributed mass models.
13. H. M. Lundblad 1991 *International Journal for Numerical Methods in Engineering* **32**, 571–594. Forced harmonic vibration of rotating beam systems in space analyzed by use of exact finite elements.
14. T. J. S. Abrahamsson and J. H. Sallstrom 1996 *Journal of Engineering for Gas Turbines Power-Transactions of the ASME* **118**(1), 86–94. A spinning finite beam element of general orientation analyzed with Rayleigh/Timoshenko/Saint-Venant theory.
15. R. L. Bielawa 1992 *Rotary Wing Structural Dynamics and Aeroelasticity* (AIAA Education Series). Washington, DC: AIAA.
16. K. J. Bathe 1982 *Finite Element Procedure in Engineering Analysis*. Englewood Cliffs, NJ: Prentice–Hall.
17. W. L. Cleghorn and B. Tabarrok 1992 *Journal of Sound and Vibration* **152**(3), 461–470. Finite element formulation of a tapered Timoshenko beam for free lateral vibration analysis.

18. J. S. Przemieniecki 1968 *Theory of Matrix Structural Analysis*. New York: McGraw–Hill.
19. F. W. Williams and W. H. Wittrick 1970 *International Journal of Mechanical Sciences* **12**, 781–791. Automatic computational procedure for calculating natural frequencies of skeletal structures.
20. W. H. Wittrick and F. W. Williams 1971 *Quarterly Journal of Mechanics and Applied Mathematics* **24**, 263–284. A general algorithm for computing natural frequencies of elastic structures.
21. W. H. Wittrick and F. W. Williams 1971 *International Union of Theoretical and Applied Mechanics Symposium on High Speed Computing of Elastic Structures, University of Liege, Liege, Belgium*. Natural vibrations of thin, prismatic flat-walled structures; pp. 563–588.
22. J. R. Banerjee and S. A. Fisher 1992 *International Journal for Numerical Methods in Engineering* **33**, 739–751. Coupled bending-torsional dynamic stiffness matrix for axially loaded beam elements.
23. J. R. Banerjee and F. W. Williams 1985 *International Journal for Numerical Methods in Engineering* **21**, 2289–2302. Exact Bernoulli–Euler dynamic stiffness matrix for a range of tapered beams.
24. F. W. Williams and W. H. Wittrick 1983 *Journal of Structural Engineering* **109**(1), 169–187. Exact buckling and frequency calculations surveyed.
25. S. M. Hashemi, M. J. Richard and G. Dhatt 1996 *Proceeding of* "*Acoustic Week in Canada* 1996", *Calgary*, *Alberta*. A Bernoulli–Euler stiffness matrix approach for vibrational analysis of linearly tapered beams; p. 87.
26. S. M. Hashemi, M. J. Richard and G. Dhatt 1997 *Proceeding of* "16*th Canadian Congress of Applied Mechanics* (*CANCAM* 1997)", *Québec*, *Québec*. A Dynamic Finite Element (DFE) formulation for free vibration analysis of centrifugally stiffened uniform beams; pp. 443–444.
27. S. M. Hashemi, M. J. Richard and G. Dhatt 1997 42*nd ASME Gas Turbine and Aeroengine Congress*, *Orlando*, *FL*, Paper No. 97-GT-500. A Bernoulli–Euler stiffness matrix approach for vibrational analysis of spinning linearly tapered beams.
28. G. Dhatt and G. Touzot 1984 *Une présentation de la méthode des éléments finis*; S. A. Maloine Éditeur. Paris: Les presses de l'Université Laval, Québec (in French); pp. 100–103.
29. B. Å. Åkesson 1976 *International Journal for Numerical Methods in Engineering* **10**, 1221–1231. PFVIBAT—a computer program for plane frame vibration analysis by an exact method.
30. P. Swannell 1973 *Theory and Practice in Finite Element Structural Analysis*. Tokyo: University of Tokyo Press. The automatic computation of the natural frequencies of structural frames using an exact matrix technique; pp. 289–309.
31. Projet REF_LEX; (in French, '**R**echerche et **E**nseignement en modélisation des structures **FLEX**ible') Professeurs BATOZ et DHATT, Division MNM/Département GM, Université de technologie de Compiegne, France.

APPENDIX: NOMENCLATURE

D = denominator in the expressions of N_1, N_2, N_3 and N_4 (shape functions)
$H_{fy}(x) = EI(x)$; flexural rigidity
H_{fy} = assumed constant average value of $H_{fy}(x)$, calculated in the middle of the member (or element)
$[K]$ = static stiffness matrix obtained by the finite element method
$[K_{DS}]$ = overall dynamic stiffness matrix obtained by the DFE method
$[K_{DS}^{\triangle}]$ = upper triangular matrix obtained from $[K_{DS}]$
$[K_{DS}]^k$ = DFE stiffness matrix

$[K_{DS}]^k_{Average}$ = first part of $[K_{DS}]$ corresponding to the uniform assumed beam element
$[K_{DS}]^k_{DEV}$ = deviatoric part of $[K_{DS}]^k$
$(K_{DSij})^k_{DEV}$ = components of $[K_{DS}]^k$; $i, j = 1, 2, 3, 4$
L = total length of the beam
$[M]$ = static mass matrix obtained by the finite element method
NE = total number of elements
$T(x)$ = centrifugal force acting along the beam
$T = (\int_{x_1}^{x_2} T(x)\,\mathrm{d}x)/(x_2 - x_1)$; assumed constant average value of $T(x)$
$T_k = \Omega^2 \int_x^{l_k} m_k(x_0 + x_k + x)\,\mathrm{d}x + T_{k-1}(0)$; centrifugal force corresponding to the element k
W_{INT} = internal virtual work
W_{EXT} = external virtual work
W^k = discretized internal virtual work corresponding to element k
W^k_{ND} = non-dimensionalized form of W^k
$\bar{l}_k = l_k/L$; non-dimensionalized length of element k
$m(x) = \rho A(x)$; mass per unit length
m_r = reference value of $m(x)$; usually chosen as $m(x)$ at one end of the beam (here, at the $x = 0$)
m = assumed constant average value of $m(x)$, calculated in the middle of the member (or element)
$\bar{m} = m/m_r$; non-dimensionalized form of m
w = displacement in the plane of vibration
x_k = distance of the element k from the centre of rotation
$\bar{x}_k = x_k/L$; non-dimensionalized x_k
$\xi = x/l_k$; elementary local coordinate, $0 \leqslant \xi \leqslant 1$
$\gamma_k = EI_k/EI_r$; non-dimensionalized form of EI_k
$\lambda^2 = m_r\Omega^2L^4/(EI_r)$; non-dimensionalized form of Ω^2
$\mu_2 = m_r\hat{\omega}^2L^4/(EI_r)$; non-dimensionalized form of $\hat{\omega}^2$
Ω = rotating speed of the beam
ω = rotary frequency
$\hat{\omega}^2 = \omega^2 + \Omega^2 \sin^2\theta$
$\tau_k = T_k/(m_r\Omega^2L^2)$; non-dimensionalized form of T_k

Indices

$(\Gamma)' = \partial\Gamma/\partial x$ or $\partial\Gamma/\partial\xi$
$(\dot{\Gamma}) = \partial\Gamma/\partial t$
$(\bar{\Gamma})$ = non-dimensionalized parameter
$(\Gamma)_{,x} = \partial\Gamma/\partial x$
$(\Gamma)_k$ = parameter corresponding to the element k
$(\Gamma)_r$ = reference parameter, here calculated for the cantilevered end